

Joint Interference Cancellation and Resource Allocation for Full-duplex Cloud Radio Access Networks

Chun-Hao Fang, Pei-Rong Li, and Kai-Ten Feng

Department of Electrical and Computer Engineering, National Chiao Tung University, Hsinchu, Taiwan
eie5577.cm03g@nctu.edu.tw, shockbowwow.cm01g@nctu.edu.tw, and ktfeng@mail.nctu.edu.tw

Abstract—In this paper, we study joint interference cancellation and resource allocation for full-duplex (FD) cloud radio access networks (C-RAN) with antenna correlation. The target is to maximize the capacity of downlink (DL) user equipments (UEs) with guaranteed quality of service (QoS) of UL UEs under the constraints of DL and uplink (UL) transmit power. Intractability of the considered problem involves non-convexity and coupling between postcoding and remote radio head (RRH) selection. To deal with the high coupling between system variables, an estimation-free self-interference (SI) cancellation (EFSC) scheme with merit of significantly reducing signaling overhead for channel estimation is proposed. The reduced signaling overhead is also derived in closed form expression. Furthermore, we propose a generalized Benders decomposition based resource allocation (GRA) algorithm, which separates the continuous and discrete variables to solve the optimization problem. With the design of a flexible utility function, the tradeoff between DL capacity and co-channel interference (CCI) can be achieved. Moreover, we identify the scenario in which antenna correlation will be beneficial for both UL and DL communications in FD C-RAN with the implementation of EFSC scheme. The effectiveness of proposed methods and theorems are verified via simulation results.

Index Terms—Full-duplex, cloud radio access networks, interference cancellation, resource allocation, antenna correlation.

I. INTRODUCTION

The feature of full-duplex (FD) communication systems is to transmit and receive signals on the same frequency band at the same time slot. Thus, it can theoretically double the spectral efficiency (SE) of half-duplex (HD) systems. In practice, the major challenge of FD systems is the strong power of self-interference (SI) from the intended downlink (DL) signals to its own uplink (UL) transmission. The SI from DL can be exceedingly large compared to the received power of UL information. The huge power difference prevents the feasibility of FD communications [1]. Fortunately, several breakthroughs in signal processing design for SI suppression have been proposed and FD prototype has been successfully presented [1, 2]. Nevertheless, owing to

the existence of residual SIs, the potential of FD systems has not been fully explored.

In order to promote the effectiveness of FD systems, several literatures [3–6] investigated channel estimation schemes for SI cancellation. In [3], a factor graph approach is proposed to jointly solve the SI cancellation and decoding problems. To further reduce the overhead of SI channel estimation, a compressed sensing based two-stage technique is developed in [4] to reduce SI power from overloading the receiver's low-noise amplifier (LNA) and ADC. Moreover, the impact of estimation error of SI channel also draws a lot of attention in recent years [5, 6]. A channel-aware multi-hop canceller is designed in [5] to jointly consider the effect on imperfect channel estimation and reconstructed errors on the estimated SI channel. In [6], the performance of an FD maximum ratio combining multiple-input multiple-output (FD-MRC-MIMO) system based on equalize-and-forward (EF) relaying with SI cancellation is analyzed under imperfect channel state information (CSI). Even though imperfect CSI on SI channel has been studied in existing literatures [3–6], how to perfectly estimate the SI channel is still an open problem and it is difficult to eliminate the residual SI completely.

To further alleviating the SI problem, several methods have been proposed to address the SI problem from the perspective of resource allocation. It has been shown that the performance of FD systems can be enhanced with efficient resource allocation algorithms [1, 2, 7, 8] by employing the cloud radio access networks (C-RAN) architecture [9–13] and adopting proper antenna selection algorithms [14, 15]. In [7], the loop interference effect in FD system is reduced by using a massive receive antenna array based on either MRC or zero-forcing (ZF) processing in multi-pair decode-and-forward relay channel. A joint beamformer design is proposed in [8] to maximize the SE subject to power constraints is considered for FD-based small cell networks, which results in higher gain over HD system. Even though various network architectures such as relay and small cells have been discussed for FD system with performance enhancement, [9] indicates that SI can be naturally suppressed with the distributed manner of remote radio head (RRH) in C-RAN. In other words, the transmitting RRH and receiving RRH can be distantly located to avoid SI in FD system. The work in

¹This work was in part funded by MOST 107-2622-8-009-020, 107-2218-E-009-047, 107-2221-E-009-058-MY3, and the National Chung-Shan Institute of Science and Technology (NCSIST), Taiwan. The corresponding author is Kai-Ten Feng.

[10, 11] derived analytical expressions to compare the average sum rate among cell association schemes as a function of both the number of RRH's antennas and the density of UL and DL RRHs.

Except for resource allocation design and C-RAN architecture, antenna selection has been shown in [14] to be an efficient method to suppress SI by avoiding the strongest components of SI channel. However, the major challenge of antenna selection is its high computational complexity when the number of antenna is increased. A computational-efficient antenna selection algorithm is proposed in [15] based on greedy approach for FD MIMO system, which can achieve almost the same system capacity as the exhaustive search algorithm. Furthermore, the impacts of antenna correlation to FD system have been discussed in [16, 17] to consider practical communication phenomenon. In [16], the performance of FD two-way massive MIMO relay systems is analyzed considering antenna correlation at both the relay and users. A closed-form expression for ergodic capacity with antenna correlation has been derived in [17] for FD system, which indicates that higher capacity can be achieved with larger cross correlation between two communication links.

In this paper, we will investigate and design joint interference cancellation and resource allocation for FD C-RAN with antenna correlation. An optimization problem is formulated to maximize the capacity of DL user equipments (UEs) by guaranteeing the quality of service (QoS) of UL UEs under the constraints of DL and UL transmit power. The formulated problem involves non-convexity and coupling between postcoding and RRH selection, which makes resource allocation design hard to be tractable. In this paper, we develop an estimation-free SI cancellation (EFSC) scheme along with a resource allocation algorithm based on the generalized Benders decomposition (GBD) [1]. Moreover, although some works discussed the outage probability and ergodic capacity of FD systems with existence of antenna correlation, it is still unclear how antenna correlation will affect the performance of resource allocation. We will investigate the scenario where antenna correlation is beneficial for both UL and DL communications, and provide significant insights on resource allocation policy when antenna correlation exists for FD C-RAN.

Furthermore, the data traffic in practical communication systems in general possesses asymmetric trends [18–21]. The asymmetric traffic would waste the radio resources and degrade its utilization in the communication networks with symmetric resource allocation. In this paper, we take asymmetric traffic property into consideration, which has been ignored in aforementioned works. The main contributions of this paper are summarized as follows.

- Without the need to perform SI channel estimation via pilot sequences, we propose the EFSC scheme by extracting the SI channel information directly from

the received signals. Thus, the signaling overhead required for channel estimation can be significantly reduced by adopting the EFSC scheme. Moreover, the reduced signaling overhead is derived in closed form, which allows us to explicitly observe how much improvement is achieved by implementing the proposed EFSC scheme.

- Based on the EFSC method for SI cancellation, we develop a GBD-based resource allocation (GRA) scheme which optimizes continuous and discrete variables separately. The bisection search method and the difference of convex function (DC) approach are adopted to solve the optimization of continuous variables. On the other hand, a flexible utility function associating a penalty term is applied for acquiring the discrete variables with the consideration of co-channel interference (CCI). The proposed GRA algorithm is designed to maximize the utility function by selecting a feasible set of RRHs considering the tradeoff between DL capacity and CCI.
- We identify the scenario in which antenna correlation will be beneficial for both UL and DL communications in FD C-RAN with the implementation of proposed EFSC scheme. The number of UL UE that can be served and the number of RRH that can be allocated for DL communications in FD C-RAN are inversely proportional to the rank of SI channel matrix. Consequently, the capacity of both UL and DL communications will be improved by increasing the number of UL UE for DL communications when antenna correlation occurs at DL RRHs due to its ability to reduce the rank of SI channel matrix. Moreover, consider the specific case with broadcast channel, by the fact that DL capacity of broadcast channel is proportional to the singular value of channel matrix, antenna correlation can still improve DL capacity in broadcast channel based on the property that correlation matrix has larger singular value than non-correlated matrix.

II. SYSTEM MODEL

A. System Scenario

Fig. 1 shows the network scenario for FD C-RAN with multiple users. The system consists of N_S single antenna RRH (SA-RRH), N_M multiple antenna RRH (MA-RRH), K mobile users and a baseband unit (BBU) pool containing several BBUs. Each MA-RRH is equipped with λ antennas. The K users employ single-antenna HD mobile communication devices to ensure low hardware complexity and will be scheduled for either UL or DL transmissions. In particular, the numbers of DL and UL UEs are denoted by K_D and K_U respectively. On the other hand, RRHs are connected to one of the BBUs via fronthaul links. Noted that BBU is a powerful computational unit, which is capable of computing the resource allocation policy for C-RAN based on the

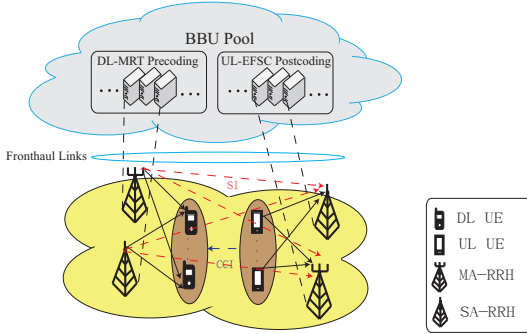


Fig. 1. Full-duplex systems in cloud radio access networks.

CSI and network environments. For the convenience of comparison, we assume that the BBU possesses full CSI information of the network except for the SI CSI. In order to acquire the SI CSI, the BBU employs minimum mean square error (MMSE) estimator. Thus, the estimated error of SI CSI will be modeled as a Gaussian distribution random variable. Furthermore, the BBU will assign either the DL transmission (DL RRH) or UL reception (UL RRH) tasks to RRHs after the resource allocation policy is determined, i.e., DL transmission and UL reception cannot be implemented on the same RRH simultaneously. Specifically, each RRH receives the control signals for resource allocation from BBU via fronthaul links. Afterwards, DL RRHs will transmit data to the K_D DL users while UL RRHs will transfer the received UL data signals via fronthaul links to the BBU to decode the information.

B. Signal Model

The received signal for the k -th DL UE y_{D_k} can be written as

$$y_{D_k} = d_{S,k} + d_{M,k} + I_{S,k} + I_{M,k} + I_{CCI,k} + n_k, \quad (1)$$

where $d_{S,k} \in \mathbb{C}$ and $d_{M,k} \in \mathbb{C}$ are the desired signals from SA-RRHs and MA-RRHs to the k -th DL UE respectively, and are given as

$$d_{S,k} = \sum_{i=1}^{N_S} \alpha_{S_i} p_{S_i,k}^{1/2} g_{D_i,k}^H v_{i,k} x_{D_k}, \quad (2)$$

$$d_{M,k} = \sum_{i=1}^{N_M} \alpha_{M_i} p_{M_i,k}^{1/2} \mathbf{g}_{D_i,k}^H \mathbf{v}_{i,k} x_{D_k}. \quad (3)$$

The parameters $\alpha_{S_i}, \alpha_{M_i} \in \{0, 1\}$ in (2) are binary indicators, where 1 indicates that the corresponding RRH implements DL transmission and 0 denotes UL reception for the RRH. $p_{S_i,k}$ and $p_{M_i,k} = \sum_{j=1}^{\lambda} p_{MA_j,i,k} / \lambda$ are respectively the allocated power from the i -th SA-RRH and i -th MA-RRH to the k -th DL UE, where $p_{MA_j,i,k}$ is the allocated power of the j -th antenna on the i -th MA-RRH to the k -th DL UE. It is considered that MA-RRHs allocate equal power to each antenna. $g_{D_i,k} \in \mathbb{C}^{\lambda}$

and $\mathbf{g}_{D_i,k} \in \mathbb{C}^{\lambda}$ are channel gain and channel vector from the i -th SA-RRH and i -th MA-RRH to the k -th DL UE, respectively. x_{D_k} indicates the data symbols transmitted to the k -th DL UE, where the power of data symbol satisfies $E\{|x_{D_k}|^2\} = 1$. Maximum ratio transmission (MRT) precoding at the i -th SA-RRH and i -th MA-RRH to the k -th DL UE are respectively denoted by $v_{i,k} \in \mathbb{C}$ and $\mathbf{v}_{i,k} = [v_{1,i,k}, \dots, v_{\lambda,i,k}] \in \mathbb{C}^{\lambda}$. It can also be written as $v_{i,k} = g_{D_i,k} \psi_{S_i,k}$ and $\mathbf{v}_{i,k} = \mathbf{g}_{D_i,k} \psi_{M_i,k}$, where $\psi_{S_i,k} \in \mathbb{C}$ and $\psi_{M_i,k} \in \mathbb{C}$ ensure that $v_{i,k}$ and $\mathbf{v}_{i,k}$ satisfy

$$E\{v_{i,k}^H v_{i,k}\} = E\{\mathbf{v}_{i,k}^H \mathbf{v}_{i,k}\} = 1. \quad (4)$$

Moreover, the parameters $I_{S,k}$ and $I_{M,k}$ in y_{D_k} are the inter-user interference (IUI) from SA-RRH and MA-RRH to the k -th DL UE respectively, and can be expressed as

$$I_{S,k} = \sum_{i=1}^{N_S} \sum_{j=1, j \neq k}^{K_D} \alpha_{S_i} p_{S_i,j}^{1/2} g_{D_i,j}^H v_{i,j} x_{D_j}, \quad (5)$$

$$I_{M,k} = \sum_{i=1}^{N_M} \sum_{j=1, j \neq k}^{K_D} \alpha_{M_i} p_{M_i,j}^{1/2} \mathbf{g}_{D_i,j}^H \mathbf{v}_{i,j} x_{D_j}. \quad (6)$$

The CCI in y_{D_k} from UL UEs to the k -th DL UE is written as

$$I_{CCI,k} = \sum_{i=1}^{K_U} p_{U_i}^{1/2} h_{C_i,k}^H x_{U_i}, \quad (7)$$

where p_{U_i} is the transmit power from the i -th UL UE and $h_{C_i,k} \in \mathbb{C}$ is the channel gain from the i -th UL UE to the k -th DL UE. $n_k \sim \mathcal{CN}(0, \sigma_k^2)$ in y_{D_k} represents the additive Gaussian noise (AWGN) at the k -th DL UE. The achievable capacity of DL transmission for the k -th DL UE in the considered scenario can be written as

$$R_{D_k} = \log_2(1 + \gamma_{D_k}), \quad (8)$$

where the received signal-to-interference-plus-noise ratio (SINR) for DL UE k (γ_{D_k}) is

$$\gamma_{D_k} = \frac{|d_{S,k}|^2 + |d_{M,k}|^2}{|I_{S,k}|^2 + |I_{M,k}|^2 + |I_{CCI,k}|^2 + \sigma_k^2}. \quad (9)$$

Note that the parameters in (9) can be obtained from y_{D_k} . Furthermore, the received signals of UL transmission for SA-RRH y_S and for MA-RRH y_M can be respectively obtained as

$$y_S = d_{U,S} + c_{S,S} + c_{M,S} + n_1, \quad (10)$$

$$y_M = \mathbf{d}_{U,M} + \mathbf{c}_{S,M} + \mathbf{c}_{M,M} + \mathbf{n}_2. \quad (11)$$

$d_{U,S}$ and $d_{U,M}$ are the received UL signals at SA-RRHs and MA-RRHs, respectively, and are expressed as

$$d_{U,S} = \sum_{k=1}^{K_U} d_{U_k,S} = \sum_{k=1}^{K_U} \sum_{j=1}^{N_S} (1 - \alpha_{S_j}) p_{U_k}^{1/2} g_{U_{k,j}} x_{U_k}, \quad (12)$$

$$d_{U,M} = \sum_{k=1}^{K_U} d_{U_k,M} = \sum_{k=1}^{K_U} \sum_{j=1}^{N_M} (1 - \alpha_{M_j}) p_{U_k}^{1/2} g_{U_{k,j}} x_{U_k}, \quad (13)$$

where $d_{U_k,S}$ and $d_{U_k,M}$ respectively indicates the received UL signals at SA-RRH and MA-RRH from the k -th UE. $g_{U_{i,j}} \in \mathbb{C}$ and $\mathbf{g}_{U_{i,j}} \in \mathbb{C}^\lambda$ are the channel gain and channel vector from the i -th UL UE to the j -th SA-RRH and j -th MA-RRH. x_{U_k} represents the data symbols sent from the k -th UL UE with the power satisfying $E\{|x_{U_k}|^2\}=1$. $c_{S,S}$, $c_{M,S}$, $c_{S,M}$, $c_{M,M}$ in y_S and \mathbf{y}_M denote the SI from SA-RRHs to SA-RRHs, MA-RRHs to SA-RRHs, SA-RRHs to MA-RRHs, and MA-RRHs to MA-RRHs repectively as follows

$$\begin{cases} c_{S,S} = \sum_{S_i,S_k} \alpha_{S_i} (1 - \alpha_{S_k}) p_{S_{i,j}}^{1/2} h_{S_{i,S_k}}^H v_{i,j} x_{D_j}, \\ c_{M,S} = \sum_{M_i,S_k} \alpha_{M_i} (1 - \alpha_{S_k}) p_{M_{i,j}}^{1/2} \mathbf{h}_{M_{i,S_k}}^H \mathbf{v}_{i,j} x_{D_j}, \\ c_{S,M} = \sum_{S_i,M_k} \alpha_{M_k} (1 - \alpha_{M_k}) p_{S_{i,j}}^{1/2} \mathbf{h}_{S_{i,M_k}}^H v_{i,j} x_{D_j}, \\ c_{M,M} = \sum_{M_i,M_k} \alpha_{M_k} (1 - \alpha_{M_k}) p_{M_{i,j}}^{1/2} \mathbf{H}_{M_{i,M_k}} \mathbf{v}_{i,j} x_{D_j}, \end{cases} \quad (14)$$

where $\sum_{x,y} = \sum_{i=1}^{N_x} \sum_{j=1}^{K_D} \sum_{k=1, k \neq i}^{N_y}$ with x and y denoting either S or M. h_{x_i,y_k} or \mathbf{h}_{x_i,y_k} are the SI channel gain from i -th x A-RRH to k -th y A-RRH. $\mathbf{H}_{M_{i,M_k}} \in \mathbb{C}^{\lambda \times \lambda}$ is the SI channel matrix from the i -th MA-RRH to k -th MA-RRH. Furthermore, n_1 and \mathbf{n}_2 in y_S and \mathbf{y}_M are written as

$$\begin{cases} n_1 = \sum_{i=1}^{N_S} (1 - \alpha_{S_i}) n_{S_i}, \\ \mathbf{n}_2 = \sum_{i=1}^{N_M} (1 - \alpha_{M_i}) \mathbf{n}_{M_i}, \end{cases} \quad (15)$$

where $n_{S_i} \sim \mathcal{CN}(0, N_0)$ and $\mathbf{n}_{M_i} \sim \mathcal{CN}(\mathbf{0}, N_0 \mathbf{I}_\lambda)$ are AWGN at SA-RRH and MA-RRH respectively. Note that both large-scale and fast fadings are considered in this work. The effect of antenna correlation incurs at the MA-RRHs. For the purpose of illustration, the channel gain and channel vector in (2) are taken as an example, which can be decomposed as

$$\begin{cases} g_{D_{i,k}} = s_{i,k}^{1/2} \rho_{i,k}, \\ \mathbf{g}_{D_{i,k}} = s_{i,k}^{1/2} \mathbf{R}_{i,k}^{1/2} \boldsymbol{\rho}_{i,k}, \end{cases} \quad (16)$$

where $s_{i,k} \in \mathbb{C}$ is the pathloss effect. $\rho_{i,k} \in \mathbb{C}$ and $\boldsymbol{\rho}_{i,k} \in \mathbb{C}^\lambda$ are the scalar and vector accounting fast fading respectively, and are usually modeled as Rayleigh distribution. $\mathbf{R}_{i,k} \in \mathbb{C}^{\lambda \times \lambda}$ is the matrix that characterizes

the antenna correlation effect at the MA-RRH as

$$\mathbf{R}_{i,k} = \begin{bmatrix} 1 & \dots & (e^{-j\theta_{ik}})^{\lambda-1} \\ \vdots & \ddots & \vdots \\ (e^{j\theta_{ik}})^{\lambda-1} & \dots & 1 \end{bmatrix}, \quad (17)$$

where θ_{ik} is randomly generated from a uniform distribution over $[0, 2\pi]$, $\forall i, k$. When linear postcoding processing is implemented after the UL signals are received, y_S and \mathbf{y}_M can be rewritten as

$$w_S y_S = w_S d_{U,S} + w_S c_{S,tot} + w_S n_1, \quad (18)$$

and

$$\mathbf{w}_M^H \mathbf{y}_M = \mathbf{w}_M^H \mathbf{d}_{U,M} + \mathbf{w}_M^H \mathbf{c}_{M,tot} + \mathbf{w}_M^H \mathbf{n}_2, \quad (19)$$

where $c_{S,tot} = c_{S,S} + c_{M,S}$ and $\mathbf{c}_{M,tot} = \mathbf{c}_{S,M} + \mathbf{c}_{M,M}$. w_S and \mathbf{w}_M are respectively the postcoding processing for the SA-RRHs and MA-RRHs. Thus, the achievable capacity of k -th UL UE can be obtained as

$$R_{U_k} = \log_2(1 + \gamma_{U_k}), \quad (20)$$

where

$$\gamma_{U_k} = \frac{|w_S d_{U_k,S}|^2 + \|\mathbf{w}_M^H \mathbf{d}_{U_k,M}\|^2}{|w_S c_{S,tot}|^2 + \|\mathbf{w}_M^H \mathbf{c}_{M,tot}\|^2 + |w_S n_1|^2 + \|\mathbf{w}_M^H \mathbf{n}_2\|^2}, \quad (21)$$

with $d_{U_k,S}$ and $\mathbf{d}_{U_k,M}$ acquired from (12) and (13).

C. Problem Formulation

In this subsection, a non-convex resource allocation problem with the consideration of asymmetric traffic characteristics in the wireless networks is formulated. The system objective is to maximize the DL capacity and guarantee QoS of UL UEs under the transmission power constraints of the DL RRHs and UL UEs. The optimization problem is expressed as follows:

$$\max_{\alpha_S, \alpha_M, \mathbf{p}_S, \mathbf{p}_M, \mathbf{p}_U, w_S, \mathbf{w}_M} R_D \quad (22a)$$

$$\text{subject to } \sum_{k=1}^{K_D} p_{S_{i,k}} \leq p_{S_{\max}}, \quad \forall i \quad (22b)$$

$$\sum_{k=1}^{K_D} p_{M_{i,k}} \leq p_{M_{\max}}, \quad \forall i \quad (22c)$$

$$p_{U_i} \leq p_{U_{\max}}, \quad \forall i \quad (22d)$$

$$R_{U_k} \geq R_{\text{req}}, \quad \forall k \quad (22e)$$

$$\alpha_{S_i}, \alpha_{M_j} \in \{0, 1\}, \quad \forall i, j \quad (22f)$$

where $R_D = \sum_{k=1}^{K_D} R_{D_k}$ and $\alpha_S, \alpha_M, \mathbf{p}_S, \mathbf{p}_M, \mathbf{p}_U$ are symbolic notations of design variables representing SA-RRH selection, MA-RRH selection, transmission power

of SA-RRH, transmission power of MA-RRH, and transmission power of UL UEs, respectively. w_S and w_M are the postcoding coefficients for the SA-RRHs and MA-RRHs, respectively. (22b), (22c), (22d) are transmission power constraints of SA-RRH, MA-RRH, and UL UEs. (22e) is the QoS constraint of k -th UL UE, and (22f) are binary indicators of RRH selection, which were explained in (2). Note that asymmetric traffic property is reflected in the optimization problem formulation, which aims to maximize capacity of DL UEs while guaranteeing minimum capacity of UL UEs. This formulation implies higher DL capacity over UL and signifies that the system will allocate resources only to DL UEs once minimum capacity requirement of UL UEs is satisfied.

III. INTERFERENCE CANCELLATION METHOD AND RESOURCE ALLOCATION ALGORITHM DESIGN

The formulated problem in (22a) is a mixed integer non-linear problem (MINLP) with non-convex objective function (22a) and non-convex constraint (22e). The combinatorial nature is due to the binary indicators in (22f). Also, the RRH selection variables α_S and α_M are coupled with postcoding coefficients w_S and w_M from R_{D_k} in (22a) and R_{U_k} (22e). In the following subsections, we will first present the proposed EFSC scheme in closed-form for SI cancellation with reduced signaling overhead. Then, the GRA algorithm is implemented by decomposing the original problem into two subproblems. The bisection search method and DC programming approach are adopted to solve the subproblem. Moreover, a utility function is designed with the consideration of the impact from CCI. It will be shown that the proposed GRA scheme can achieve tradeoff between DL throughput and CCI.

A. Proposed Estimation-Free SI Cancellation (EFSC) Scheme

Our main goal is to design a feasible postcoding scheme for receive antennas at RRHs in order to perfectly eliminate the SI as well as keeping the desired signals unchanged. For the convenience of illustration, the numbers of transmit antenna and receive antenna are represented by N_t and N_r respectively after RRH selection. N_t and N_r can be determined by initialization procedure of proposed GRA algorithm, which will be mentioned in Subsection III-B. The received signals at RRHs can be rewritten from y_S and y_M as

$$\mathbf{y} = \mathbf{G}\mathbf{x}_{UL} + \mathbf{H}\mathbf{x}_{DL} + \mathbf{n}, \quad (23)$$

where $\mathbf{G} \in \mathbb{C}^{N_r \times K_U}$ and $\mathbf{H} \in \mathbb{C}^{N_r \times N_t}$ are UL channel matrix and SI channel matrix respectively. $\mathbf{x}_{UL} \in \mathbb{C}^{K_U}$ and $\mathbf{x}_{DL} \in \mathbb{C}^{N_t}$ can be represented as

$$\mathbf{x}_{UL} = \left[p_{U_1}^{1/2} x_{U_1}, \dots, p_{U_{K_U}}^{1/2} x_{U_{K_U}} \right]^H, \quad (24)$$

with $p_{U_1}, \dots, p_{U_{K_U}}$ sharing the same definition as p_{U_k} in $d_{U,S}$ and $\mathbf{d}_{U,M}$.

$$\mathbf{x}_{DL} = \left[\sum_{j=1}^{K_D} p_{D_{1,j}}^{1/2} v_{D_{1,j}} x_{D_j}, \dots, \sum_{j=1}^{K_D} p_{D_{N_t,j}}^{1/2} v_{D_{N_t,j}} x_{D_j} \right]^H, \quad (25)$$

where

$$\begin{cases} p_{D_{i,k}} = p_{S_{i,k}}, & \forall i \in \mathcal{S} \\ p_{D_{i,k}} = p_{MA_{i,k}}, & \forall i \in \mathcal{M} \end{cases} \quad (26)$$

with $i \in \mathcal{S}$ indicating that the antenna is from SA-RRHs and $i \in \mathcal{M}$ meaning that from MA-RRHs. $v_{D_{i,j}} \in \mathbb{C}$ is the MRT processing of the i -th DL antenna to j -th UE. $\mathbf{n} \sim \mathcal{CN}(0, N_0 \mathbf{I}_{N_r})$ is the AWGN. After processed by the postcoder, the received signals can be rewritten as

$$\mathbf{W}\mathbf{y} = \mathbf{W}\mathbf{F}\tilde{\mathbf{x}} + \mathbf{W}\mathbf{n}, \quad (27)$$

where $\mathbf{F} = [\mathbf{G} \quad \mathbf{H}]$, and $\tilde{\mathbf{x}} = [\mathbf{x}_{UL}^T \quad \mathbf{x}_{DL}^T]^T$. The desired \mathbf{W} is expected to satisfy the condition

$$\mathbf{WF} = [\mathbf{G} \quad \mathbf{0}], \quad (28)$$

which means that the SI can be perfectly nulled. The postcoding design in proposed EFSC scheme is provided in the following theorem.

Theorem 1 Given UL CSI \mathbf{G} matrix, the SI in the FD C-RAN can be completely eliminated by the proposed EFSC scheme with postcoder \mathbf{W} constructed as

$$\mathbf{W} = \mathbf{G}(\mathbf{G}^H \mathbf{R}_F^\dagger \mathbf{G})^{-1} \mathbf{G}^H \mathbf{R}_F^\dagger, \quad (29)$$

where $\mathbf{R}_F = \mathbf{R}_y - N_0 \mathbf{I}_{N_r} = E[\mathbf{y}\mathbf{y}^H] - N_0 \mathbf{I}_{N_r}$.

Proof: Please see Appendix A. \blacksquare

Notice that concept of the proposed EFSC scheme is to project the received signal to the direction of UL channel's subspace. SI can be effectively eliminated after projection when the subspaces of UL channel and SI channel are disjoint with each other by the fact that the received signal \mathbf{y} at UL RRHs is comprised of the components from subspace of UL channel and subspace of SI channel. Hence, the proposed EFSC method is only slightly affected by the accuracy of UL CSI, which will be demonstrated in Section V since the subspace of the obtained UL CSI does not overlap with subspace of SI channel. The disjoint between these two subspaces means that the column spaces spanned by \mathbf{G} and \mathbf{H} should be linearly independent with each other. To ensure linear independence of column spaces, the number of rows of matrix \mathbf{F} should be greater or equal to the number of columns of matrix \mathbf{F} [22]. Thus, the condition $N_r \geq N_t + K_U$ should be satisfied, where K_U represents the number of UL UE. Moreover, pilot sequence is well-adapted to implement channel estimation [7, 23] in practical systems. When \mathbf{W} is constructed from $\mathbf{GG} = \mathbf{G}(\mathbf{G}^H \mathbf{Q}_H^\perp \mathbf{G})^{-1} \mathbf{G}^H \mathbf{Q}_H^\perp$, with $\mathbf{Q}_H^\perp = \mathbf{I} - \mathbf{H}(\mathbf{H}^H \mathbf{H})^{-1} \mathbf{H}^H$, both UL CSI and SI CSI estimation will

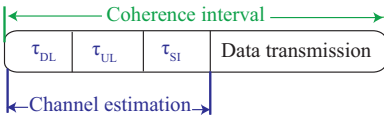


Fig. 2. Illustration of coherence interval.

be implemented via the transmission of pilot sequences among DL RRHs and UL RRHs which will occupy a portion of coherence interval for data transmission as shown in Fig. 2. Note that τ_{DL}, τ_{UL} and τ_{SI} in Fig. 2 are the lengths of coherence interval for DL, UL and SI CSI estimation respectively. When \mathbf{W} is constructed as $\mathbf{G}(\mathbf{G}^H \mathbf{R}_F^\dagger \mathbf{G})^{-1} \mathbf{G}^H \mathbf{R}_F^\dagger$, on the other hand, SI CSI estimation via the transmission of pilot sequences is not required since the proposed EFSC scheme is able to obtain \mathbf{R}_F^\dagger , which is equal to $\mathbf{Q}_{\mathcal{H}}^\perp$ in $\bar{\mathbf{G}}$. Due to the fact that EFSC scheme enables the construction of \mathbf{W} without occupying any part of coherence interval, the EFSC method can effectively reduce the signaling overhead of CSI estimation. The coherence interval originally used for SI CSI estimation, i.e., τ_{SI} in Fig. 2, can be utilized for data transmission. Hence, the capacity improvement can be achieved by employing the proposed EFSC scheme. Calculation of the reduced pilot sequence overhead τ_{SI} by adopting the EFSC method is provided as follows.

Theorem 2 Let τ_{SI} denote the length of pilot sequences (in symbols) saved by proposed EFSC scheme when adopting channel estimation method in [7, 23], the following inequality will be satisfied:

$$\tau_{SI} \geq N_S(N_\lambda + N_M), \quad (30)$$

where N_S and N_M are the numbers of SA-RRH and MA-RRH, respectively, λ is the antenna number in each MA-RRH and N_λ = N_Mλ.

Proof : As shown in Fig. 2, a part of coherence interval will be used for channel estimation where τ_{DL}, τ_{UL} and τ_{SI} are the intervals for DL channel, UL channel and SI channel estimation respectively. With the implementation of EFSC scheme, the overhead for SI channel estimation can be reduced and the interval for data transmission will be increased. Thus, only the length of τ_{SI} will be focused in this proof. Moreover, the length of τ_{SI} can be further decomposed as τ_{SI} = τ_{SI_{S,S}} + τ_{SI_{S,M}} + τ_{SI_{M,S}} + τ_{SI_{M,M}}, where τ_{SI_{x,y}} means the length of interval for SI channel estimation between xA-RRHs and yA-RRH with x, y denoting either S or M. However, SI channel estimation during τ_{SI_{S,S}} and τ_{SI_{M,M}} requires concurrent transmission and reception of pilot sequences, which indicates that existing channel estimation methods [7, 23] cannot be directly applied. Since SI channel estimation procedure in τ_{SI_{S,S}} and τ_{SI_{M,M}} are out of scope of this paper, only the length of τ_{SI_{S,M}} and τ_{SI_{M,S}} will be discussed here. Hence, the length τ_{SI_{S,M}} + τ_{SI_{M,S}} is recognized as lower bound

of original signaling overhead for SI CSI estimation. In addition, since the proposed EFSC scheme allows FD C-RAN to estimate SI CSI without occupying any part of coherence interval, τ_{SI_{S,M}} + τ_{SI_{M,S}} can also be regarded as lower bound of saved overhead by the proposed scheme.

During interval τ_{SI_{S,M}}, all SA-RRHs will transmit their pilot sequences of τ_{SI_{S,M}} symbols to MA-RRHs. After the transmission of pilot sequence, the received pilot matrices at the *i*-th MA-RRHs can be written as

$$\begin{aligned} \mathbf{y}_{S,M_i} &= (\tau_{SI_{S,M}} p_{PS,M})^{1/2} \mathbf{H}_{S,M_i} \Psi_{S,M_i} \\ &\quad + (\tau_{SI_{S,M}} p_{PS,M})^{1/2} \sum_{j=1, j \neq i}^{N_M} \mathbf{H}_{S,M_i} \Psi_{S,M_j}, \end{aligned} \quad (31)$$

where p_{PS,M} is the power of pilot sequence, Ψ_{S,M_i} ∈ ℂ^{N_S × τ_{SI_{S,M}}} is the pilot sequences received by the *i*-th MA-RRH, and H_{S,M_i} ∈ ℂ^{N_M × N_S} is the channel matrix between the *i*-th MA-RRH and other SA-RRHs. Since all pilot sequences should be pairwisely orthogonal, i.e., Ψ_{S,M_i}Ψ_{S,M_i}^H = I_{N_S}, Ψ_{S,M_j}Ψ_{S,M_j}^H = I_{N_S}, and Ψ_{S,M_i}Ψ_{S,M_j}^H = 0_{N_S}, the number of column of each pilot sequences in y_{S,M_i} should be large enough to provide rank for the satisfaction of pairwisely orthogonal condition [22]. Hence, the following inequality must be satisfied:

$$\tau_{SI_{S,M}} \geq N_S N_M. \quad (32)$$

Moreover, the received pilot sequences at the *i*-th SA-RRHs during τ_{SI_{M,S}} can be written as

$$\begin{aligned} \mathbf{y}_{M,S_i} &= (\tau_{SI_{M,S}} p_{PM,S})^{1/2} \mathbf{h}_{M,S_i}^H \Psi_{M,S_i} \\ &\quad + (\tau_{SI_{M,S}} p_{PM,S})^{1/2} \sum_{j=1, j \neq i}^{N_S} \mathbf{h}_{M,S_i}^H \Psi_{M,S_j}, \end{aligned} \quad (33)$$

where p_{PM,S} is the power of pilot sequence, Ψ_{M,S_i} ∈ ℂ^{N_Mλ × τ_{SI_{M,S}}} is the pilot sequences received by the *i*-th SA-RRH, and h_{S,M_i} ∈ ℂ^{N_M} is the channel vector between the *i*-th SA-RRH and other MA-RRHs. By similar derivation techniques, τ_{SI_{M,S}} should satisfy the inequality

$$\tau_{SI_{M,S}} \geq N_S N_M \lambda. \quad (34)$$

The proof is completed by the fact τ_{SI} ≥ τ_{SI_{M,S}} + τ_{SI_{S,M}} = N_S(N_Mλ + N_M) = N_S(N_λ + N_M). ■

With the derivation of saved signaling overhead for SI channel estimation, we can provide capacity improvement by adopting EFSC scheme as follows.

Corollary 1 Let the total capacity of FD C-RAN when proposed EFSC scheme is used and not used as C₁ and C₂, respectively, the following equality will be satisfied:

$$C_1 = \frac{T - \tau_{DL} - \tau_{UL}}{T - \tau_{SI} - \tau_{DL} - \tau_{UL}} C_2, \quad (35)$$

where T is the length of coherence intervals. τ_{DL} and τ_{UL} are the intervals for DL channel and UL channel

estimation, respectively. τ_{SI} is the saved length of pilot sequence from EFSC scheme.

Proof : As shown in Fig. 2, during each coherence interval, $\tau_{\text{DL}} + \tau_{\text{UL}} + \tau_{\text{SI}}$ symbols are spent for channel estimation and the remaining interval is used for payload data transmission [7]. Thus, the total capacity of FD C-RAN when EFSC scheme is not adopted (C_2) and adopted (C_1) can be written as

$$C_2 = \frac{T - \tau_{\text{DL}} - \tau_{\text{UL}} - \tau_{\text{SI}}}{T} (R_U + R_D), \quad (36)$$

and

$$C_1 = \frac{T - \tau_{\text{DL}} - \tau_{\text{UL}}}{T} (R_U + R_D). \quad (37)$$

Result of Corollary 1 can be obtained by combining C_2 and C_1 , which completes the proof. ■

B. Proposed GBD-based Resource Allocation (GRA) Algorithm

Different approaches, including branch-and bound and outer approximation [24, 25], for solving MINLP can be adopted to obtain solution for our considered resource allocation problem in (22). In this paper, we proposed the GRA scheme based on the concept of GBD method [1]. The benefit of GBD is that it exploits the particular problem structure and leads to simple subproblems in each iteration. GBD can be used to handle the constraints involving binary optimization variables, i.e., (22e), (22f) in (22), by decomposing the problem into two subproblems: (a) *primal problem*, which is a non-convex problem involving continuous optimization variables; and (b) *master problem*, which is the mixed integer linear programming (MILP) involving the discrete variables. Specifically in our case, the primal problem is solved for a given set of α_S and α_M and will yield the upper bound for problem in (22). On the other hand, the solution of master problem will provide a lower bound of the original problem. The proposed GRA algorithm will solve the primal and master problems iteratively until the difference of two subproblems converges, which is described as follows.

1) Solution of Primal Problem in the i -th iteration:

With the implementation proposed EFSC scheme and given the result of RRH selection, the primal problem can be formulated as

$$\max_{\mathbf{p}_D, \mathbf{p}_U} R'_D \quad (38a)$$

subject to (22d)

$$\sum_{k=1}^{K_D} p_{D,i,k} \leq p_{S,\max}, \quad \forall i \in \mathcal{S} \quad (38b)$$

$$\sum_{k=1}^{K_D} p_{D,i,k} \leq p_{M,\max}, \quad \forall i \in \mathcal{M} \quad (38c)$$

$$R'_{U_k} \geq R_{\text{req}}, \quad \forall k \quad (38d)$$

Algorithm 1: Bisection Search Method

```

1: Initialization:
  1) Set iteration index  $k$ 
  2) Set the threshold of convergence  $\epsilon_1$ 
  3) Initialize  $p_{U_i}^a(0) = p_{U,\max}$ ,  $p_{U_i}^b(0) = 0$ ,
      $p_{U_i}(0) = \frac{p_{U_i}^a + p_{U_i}^b}{2}$ ,  $\forall i = 1, \dots, K_U$ 
2: repeat
3:   if (38d) is satisfied then
4:      $p_{U_i}^a(k) = p_{U_i}(k-1)$ ,
      $p_{U_i}^b(k) = p_{U_i}^b(k-1)$ ,
      $\forall i = 1, \dots, K_U$ 
5:   else
6:      $p_{U_i}^a(k) = p_{U_i}^a(k-1)$ ,
      $p_{U_i}^b(k) = p_{U_i}^b(k-1)$ ,
      $\forall i = 1, \dots, K_U$ 
7:   end if
8:    $k = k + 1$ 
9: until  $|p_{U_i}^a(k) - p_{U_i}^b(k)| \leq \epsilon_1$ 

```

where $R'_D = \sum_{k=1}^{K_D} R'_{D,k} = \sum_{k=1}^{K_D} \log_2(1 + \gamma'_{D,k})$. For the brevity of illustration, $\gamma'_{D,k}$ is written as

$$\gamma'_{D,k} = \frac{\left| \sum_{i \in \mathcal{T}} p_{D,i,k}^{1/2} g_{D,i,k} v_{D,i,k} \right|^2}{\bar{\xi}_h + |I_{\text{CCI},k}|^2 + \sigma_k^2}, \quad (39)$$

with

$$\bar{\xi}_h = \left| \sum_{i \in \mathcal{T}} \sum_{j=1, j \neq k}^{K_D} p_{D,i,j}^{1/2} g_{D,i,k} v_{D,i,j} \right|^2. \quad (40)$$

\mathcal{T} is the set of DL antennas after RRH selection. The corresponding channel gain between the i -th DL antenna and k -th DL UE is denoted by $g_{D,i,k}$. The achievable capacity of the k -th UL UE in (38d) is $R'_{U_k} = \log_2(1 + \gamma'_{U_k})$, where γ'_{U_k} is written as

$$\gamma'_{U_k} = \frac{\left| \sum_{j \in \mathcal{R}} p_{U_k}^{1/2} g_{U_k,j} \right|^2}{\|\mathbf{W}\|^2 \|\mathbf{n}_U\|^2}. \quad (41)$$

Note that \mathcal{R} in γ'_{U_k} is the set of receive antennas after RRH selection. $\mathbf{n}_U \sim \mathcal{CN}(0, N_0 \mathbf{I}_{|\mathcal{R}|})$ is the AWGN at receive antennas. The corresponding channel gain between the k -th UL UE and the j -th UL antenna is denoted by $g_{U_k,j}$. Notice that $g_{D,i,k}$ and $g_{U_k,j}$ represent channel gain between antenna and UE after RRHs are selected, which is different from the definition of $g_{D,i,k}$ and $g_{U_k,j}$. Since γ'_{U_k} is only a function of UL UE's transmission power, the constraint (22d) can be satisfied by adjusting p_{U_k} through the bisection search method, which is summarized in Algorithm 1. The bisection search method has been shown to be a solution-finding method with short convergent time and improved accuracy [26, 27]. The concept of bisection search method is to repeatedly bisect an interval and then select a subinterval, where a feasible solution

must lie in the subinterval. Consequently, the primal problem in (38) can be simplified as

$$\begin{aligned} \max_{\boldsymbol{\beta}_{\text{D}}} \quad & (38a) \\ \text{subject to} \quad & (38b), (38c). \end{aligned}$$

Since (38a) is a non-convex function, the DC approach will be applied to transform the problem. Note that the DC scheme has been widely adopted to tackle the non-convex problem with more robust and efficient manner compared to other methods [28, 29]. By adopting the DC approach and let $\beta_{i,j} = \log p_{\text{D},i,j}$, the achievable DL capacity R'_{D} in (38a) can be transformed into

$$R'_{\text{D}} = f(\boldsymbol{\beta}) - h(\boldsymbol{\beta}), \quad (43)$$

where

$$f(\boldsymbol{\beta}) = \sum_{k=1}^{K_{\text{D}}} \log_2 \left(\xi_f + |I_{\text{CCI},k}|^2 + |\sigma_k|^2 \right), \quad (44)$$

and

$$h(\boldsymbol{\beta}) = \sum_{k=1}^{K_{\text{D}}} \log_2 \left(\xi_h + |I_{\text{CCI},k}|^2 + |\sigma_k|^2 \right), \quad (45)$$

with

$$\xi_f = \sum_{i \in \mathcal{T}} \sum_{j=1}^{K_{\text{D}}} e^{\beta_{i,j}} |g_{\mathcal{D},i,j} v_{\text{D},i,j}|^2, \quad (46)$$

and

$$\xi_h = \sum_{i \in \mathcal{T}} \sum_{\substack{j=1, j \neq k}}^{K_{\text{D}}} e^{\beta_{i,j}} |g_{\mathcal{D},i,j} v_{\text{D},i,j}|^2. \quad (47)$$

Thus, the optimization problem can be expressed as

$$\max_{\boldsymbol{\beta}} \quad f(\boldsymbol{\beta}) - h(\boldsymbol{\beta}) \quad (48a)$$

$$\text{subject to} \quad \sum_{k=1}^{K_{\text{D}}} e^{\beta_{i,k}} \leq p_{\text{S},\text{max}}, \quad \forall i \in \mathcal{S} \quad (48b)$$

$$\sum_{k=1}^{K_{\text{D}}} e^{\beta_{i,k}} \leq p_{\text{M},\text{max}}. \quad \forall i \in \mathcal{M} \quad (48c)$$

It can be observed that the optimization problem in (48) becomes convex with the log-sum-exp function by adopting the DC structure. Hence, the problem can be solved by approximating $f(\boldsymbol{\beta})$ in the $\boldsymbol{\beta}$ domain through the sequential convex approximation based on first-order Taylor expansion as

$$f(\boldsymbol{\beta}) \approx f(\boldsymbol{\beta}^j) + \nabla f^T(\boldsymbol{\beta}^j)(\boldsymbol{\beta} - \boldsymbol{\beta}^j), \quad (49)$$

where $\boldsymbol{\beta}^h$ is an approximate solution at the h -th iteration, and $\nabla f(\boldsymbol{\beta}^h)$ is the gradient of $f(\boldsymbol{\beta})$ at $\boldsymbol{\beta}$ as

$$\nabla f(\boldsymbol{\beta}^j) = \left(\frac{\partial f(\boldsymbol{\beta}^j)}{\partial \beta_{l,k}} \right)^T, \quad \forall l, k. \quad (50)$$

Algorithm 2: Iterative DC Algorithm

- 1: Initialization:
 - 1) Set iteration index h
 - 2) Set the threshold of convergence ϵ_2
 - 3) Initialize $\boldsymbol{\beta}^0$
 - 2: **repeat**
 - 3: Solve (52) and denote the optimal solution as $\boldsymbol{\beta}^*$
 - 4: Update $\boldsymbol{\beta}^* = \boldsymbol{\beta}^{h+1}$
 - 5: $h = h + 1$
 - 6: **until** $|\boldsymbol{\beta}^{h+1} - \boldsymbol{\beta}^h| \leq \epsilon_2$
-

Note that $\nabla f(\boldsymbol{\beta}^h)$ is a column vector with $|\mathcal{T}|K_{\text{D}}$ elements, where $|\mathcal{T}|$ is the cardinality of set \mathcal{T} . Each element of $\nabla f(\boldsymbol{\beta}^h)$ can be computed as

$$\frac{\partial f(\boldsymbol{\beta}^h)}{\partial \beta_{l,k}} = \frac{e^{\beta_{l,k}^h} |g_{\mathcal{D},l,k} v_{\text{D},l,k}|^2}{\left(\Psi_f + |I_{\text{CCI},k}|^2 + |\sigma_k|^2 \right) \ln 2}. \quad (51)$$

By substituting $f(\boldsymbol{\beta}^h)$, $\nabla f^T(\boldsymbol{\beta}^h)$ and (51), the optimization problem in (48) can be written as

$$\max_{\boldsymbol{\beta}} \quad f(\boldsymbol{\beta}^h) + \nabla f^T(\boldsymbol{\beta}^h)(\boldsymbol{\beta} - \boldsymbol{\beta}^h) - h(\boldsymbol{\beta}) \quad (52a)$$

subject to (48b), (48c).

Notice that (52a) is a concave function since it is the addition of a line and a concave functions, whereas (48b), (48c) are convex. Thus, the problem in (52) can be solved by standard optimization solvers, e.g., CVX. The proposed iterative DC algorithm for solving the problem in (52) is summarized in Algorithm 2.

2) *Solution of Master Problem in the i -th iteration:* We are ready to formulate the master problem, which utilizes the solution of primal problem as stated in previous subsection. The master problem in the i -th iteration is given as

$$\max_{\boldsymbol{\alpha}_{\text{S}}, \boldsymbol{\alpha}_{\text{M}}} \quad \mathcal{U}_{\text{S}} + \mathcal{U}_{\text{M}} \quad (53a)$$

subject to (22f),

$$\sum_{i=1}^{N_{\text{S}}} (1 - 2\alpha_{\text{S},i}) + \sum_{i=1}^{N_{\text{M}}} (1 - 2\alpha_{\text{M},i}) \Lambda \geq K_{\text{U}}, \quad (53b)$$

where the utility functions \mathcal{U}_{S} and \mathcal{U}_{M} are

$$\begin{cases} \mathcal{U}_{\text{S}} = \chi_{\text{S}} \left(\sum_{k=1}^{K_{\text{D}}} |g_{\mathcal{D},i,k}| - V_1 \sum_{k=1}^{K_{\text{U}}} p_{\text{U},k} |g_{\text{U},k,i}| \right), \\ \mathcal{U}_{\text{M}} = \chi_{\text{M}} \left(\sum_{k=1}^{K_{\text{D}}} \|g_{\mathcal{D},i,k}\| - V_2 \sum_{k=1}^{K_{\text{U}}} p_{\text{U},k} \|g_{\text{U},k,i}\| \right). \end{cases} \quad (54)$$

$\chi_{\text{S}} = \sum_{i=1}^{N_{\text{S}}} \alpha_{\text{S},i}$ and $\chi_{\text{M}} = \sum_{i=1}^{N_{\text{M}}} \alpha_{\text{M},i}$. The utility functions can be considered as the tradeoff between DL capacity and CCI through the adjustment of parameters $V_1, V_2 \geq 0$. Specifically, if V_1 and V_2 are both with larger values, the resultant UL channel will possibly possess better quality. The constraint (38d) will be easily

satisfied without transmitting too much power from UL UEs. On the other hand, if both parameters are small, the resultant UL channel might have poor quality. UL UEs will have to increase their transmission power to fulfill the requirement in (38d) in the next iteration, which will result in large CCI. (53b) is obtained from the inequality $\sum_{i=1}^{N_S}(1 - \alpha_{S_i}) + \sum_{i=1}^{N_M}(1 - \alpha_{M_i})\Lambda \geq \sum_{i=1}^{N_S}\alpha_{S_i} + \sum_{i=1}^{N_M}\alpha_{M_i}\Lambda + K_U$, which is a variant of $N_r \geq N_t + K_U$. This constraint ensures that the subspaces spanned by the UL channel and SI channel are disjoint and limits the number of DL/UL RRH and transmit/receive antenna after RRH selection. The parameter Λ can be regarded as the multiplexing gain provided by MA-RRHs to the UEs. $\Lambda = 1$ corresponds to the existence of antenna correlation; while $\Lambda = \lambda$ indicates that there is no antenna correlation at MA-RRHs. The master problem in (53) is a MILP and can be solved by standard numerical solvers such as Mosek [30] and Gruobi [31].

3) *Proposed GRA Algorithm:* The proposed GRA algorithm is summarized in Algorithm 3 and is implemented in a repeated loop. After the basic parameters and the result of RRH selection are initialized, the primal solution is solved via Algorithms 1 and 2. Then an intermediate resource allocation policy $\Phi'(i)$ and an intermediate objective function value $f(i)$ are obtained. Moreover, the performance upper bound $UB(i)$ will be updated if the computed objective value is the lowest across all iterations. On the other hand, another intermediate resource allocation policy $\tilde{\Phi}(i)$ and performance lower bound $LB(i)$ are acquired after the master problem is solved by the standard MILP solver. The algorithm will stop when the difference between the i -th upper bound and i -th lower bound is smaller than a predefined threshold $\epsilon \geq 0$. Notice that when both primal and master problems can be solved in each iteration, the proposed GRA algorithm is guaranteed to converge to the optimal solution [1, 24].

4) *Convergence Analysis:* According to [1], the GBD method can achieve global optimum when the proposed algorithm converges. Hence, we will illustrate optimality of proposed GRA algorithm by discussing the convergence of each algorithm in primal and master problems. For Algorithm 1, it terminates when the difference $|p_{U_i}^a(k) - p_{U_i}^b(k)|$ is smaller than an arbitrarily small threshold ϵ_1 . It can be seen that the difference $|p_{U_i}^a(1) - p_{U_i}^b(1)|$ and $|p_{U_i}^a(k) - p_{U_i}^b(k)|$ are smaller than $\frac{p_{U_{\max}}}{2}$ and $\frac{p_{U_{\max}}}{2^k}$ respectively after the first and k -th iteration of Algorithm 1. Due to the fact that maximum transmission power of UL UE $p_{U_{\max}}$ is finite and $|p_{U_i}^a(k) - p_{U_i}^b(k)| \rightarrow 0$ when $k \rightarrow \infty$, the proposed Algorithm 1 will always converge when k is sufficiently large. For Algorithm 2, it can be seen that after the p -th iteration, the objective

Algorithm 3: Proposed GRA Algorithm

- 1: Initialization:
 - 1) Set iteration index i , threshold of convergence ϵ and the maximum number of iterations L_{\max}
 - 2) Initialize the upper and lower bounds of the objective function $UB(0) = \infty$, $LB(0) = -\infty$
 - 3) Initialize the result of RRH selection α_S, α_M by randomized selection under the constraint (53b)
 - 2: **repeat**
 - 3: Solve the primal problem (38) according to Algorithms 1 and 2
 - 4: Obtain intermediate resource allocation policy $\Phi'(i) = \{p_U, p_D\}$ and intermediate objective function value $f(i)$
 - 5: The upper bound $UB(i)$ is updated with $UB(i) = \min\{UB(i-1), f(i)\}$
 - 6: Solve the master probelm (53) and obtain obtain intermediate resource allocation policy $\tilde{\Phi}(i) = \{\alpha_S, \alpha_M\}$
 - 7: Obtain the value of lower bound $LB(i)$
 - 8: **if** $|UB(i) - LB(i)| \leq \epsilon$ **then**
 - 9: **return** $\{\Phi_{\text{current}}\} = \{\Phi'(i), \tilde{\Phi}(i)\}$
 - 10: **else**
 - 11: $i = i + 1$
 - 12: **end if**
 - 13: **until** $i = L_{\max}$
-

function (48a) can be written as

$$\begin{aligned} & f(\beta^p) - h(\beta^p) \\ &= f(\beta^p) + \nabla f^T(\beta^p)(\beta^p - \beta^p) - h(\beta^p) \\ &\stackrel{(a)}{\leq} f(\beta^p) + \nabla f^T(\beta^p)(\beta^{p+1} - \beta^p) - h(\beta^{p+1}) \\ &\stackrel{(b)}{\leq} f(\beta^{p+1}) - h(\beta^{p+1}), \end{aligned} \quad (55)$$

where the inequality (a) follows from the fact that β^{p+1} is the optimal solution of problem (52a) at the p -th iteration. Inequality (b) follows from the convexity of $f(\beta)$. Specifically, for any given β , $f(\beta) \geq f(\beta^p) + \nabla f^T(\beta^p)(\beta - \beta^p)$. From the above inequalities, the objective value of (48) is improved after each iteration. Hence, β^h in Algorithm 2 always converges because the objective value of (48) is finite and monotonically increasing sequences with upper bounds. For master problem, since total number of RRH in FD C-RAN is finite, it can be seen that combination of RRH selection result is also finite. Hence, there exists a unique RRH selection for each allocation result of primal problem that will maximize utility functions \mathcal{U}_S and \mathcal{U}_M . This unique RRH selection result ensures the convergence of master problem.

IV. IMPACT OF ANTENNA CORRELATION

In this section, we will evaluate the impact from antenna correlation to system performance by comparing

correlated and non-correlated MA-RRHs. The scenario in which antenna correlation is beneficial for UL and DL communications is identified via mathematical derivation. We will firstly define four extreme scenarios of RRH selection to illustrate the impact from antenna correlation on DL and UL communications by discussing the maximum number of UL UE that can be served in each scenario as follows. (1) **SDSU**: Only SA-RRHs are selected as DL RRHs and UL RRHs. (2) **MDSU**: MA/SA-RRHs are selected as DL/UL RRHs respectively. (3) **SDMU**: SA/MA-RRHs are selected as DL/UL RRHs respectively. (4) **MDMU**: Only MA-RRHs are selected as DL RRHs and UL RRHs.

The following two assumptions are made to provide fair comparison with the consideration of antenna correlation.

Assumption 1 Antenna correlation happens at MA-RRHs with correlation matrix represented as $\mathbf{R}_{i,k}$. Thus, antenna correlation will exist in MDSU, SDMU and MDMU scenarios.

Assumption 2 Let the number of DL RRHs and UL RRHs in SDSU, MDSU, SDMU, and MDMU be denoted by N_{T_1} , N_{R_1} , N_{T_2} , N_{R_2} , N_{T_3} , N_{R_3} , N_{T_4} and N_{R_4} respectively. The number of total transmit antenna are equal in four scenarios, i.e., $N_{T_1} = N_{T_2}\lambda = N_{T_3} = N_{T_4}\lambda$. The number of total receive antenna are also equal in four scenarios, i.e., $N_{R_1} = N_{R_2} = N_{R_3}\lambda = N_{R_4}\lambda$.

With the above definitions and assumptions, the comparison of the four RRH selection results is provided as follows.

Theorem 3 Under Assumptions 1 and 2, the MDSU scenario can serve the largest number of UL UEs among these four scenarios.

Proof : Let the number of UL UE that FD C-RAN can serve in SDSU, MDSU, SDMU and MDMU be denoted by K_{U_1} , K_{U_2} , K_{U_3} and K_{U_4} respectively. To effectively eliminate the SI in the FD C-RAN, the subspace spanned by the SI channel \mathcal{H} and UL channel \mathcal{G} has to be disjoint to each other. Thus, the following inequality should be satisfied $K_{U_m} + N_{T_m} \leq N_{R_m}, \forall 1 \leq m \leq 4$. Based on Assumption 2, the following relationships can be obtained: $N_{R_2} = N_{R_1} \geq N_{R_3} = N_{R_4}$, and $N_{T_1} = N_{T_3} \geq N_{T_2} = N_{T_4}$. Compared with the other three scenarios, it can be seen that Scenario 2 MDSU with the largest N_{R_2} and the smallest N_{T_2} can serve the largest number of UL UE K_{U_2} . This completes the proof. ■

Note that if Assumption 1 does not hold, i.e., when the antenna correlation does not exist at MA-RRHs, inequality for MDSU, SDMU, MDMU should be modified as $K_{U_n} \leq N_{R_n} - N_{T_n}\lambda, \forall 2 \leq n \leq 4$. From the above description, it can be seen that when scenario changes from SDSU to MDSU with the existence of antenna correlation, the condition $K_{U_2} \geq K_{U_1}$ holds due to the fact that $N_{R_2} = N_{R_1}$ and $N_{T_2} \leq N_{T_1}$, i.e., the occurrence of antenna correlation at DL RRHs makes MDSU able to

serve more UL UE than SDSU. On the other hand, when scenario changes from SDSU to SDMU with antenna correlation, the condition $K_{U_3} \leq K_{U_1}$ holds owing to the fact that $N_{R_3} \leq N_{R_1}$ and $N_{T_3} = N_{T_1}$, i.e., antenna correlation at UL RRHs provide SDSU to serve more UL UE than SDMU. In other words, the occurrence of antenna correlation at DL RRHs will be beneficial for enhancing system performance; while that at UL RRHs will be detrimental which should be avoided. Consequently, the following discussion will focus on MDSU scenario by comparing system performance with and without antenna correlation at MA-RRHs, which is defined as follows

(1) **MDSU-NC**: There is no antenna correlation at MA-RRHs and the corresponding correlation matrix becomes an identity matrix in MDSU scenario. (2) **MDSU-C**: There exists antenna correlation at MA-RRHs and the corresponding correlation matrix is represented as $\mathbf{R}_{i,k}$ in MDSU scenario.

A. Improvement of UL Capacity

First of all, the number of UL UE that the entire FD C-RAN can serve in MDSU-NC and MDSU-C are compared and summarized in the following theorem.

Theorem 4 Consider equal number of DL RRH for MDSU-NC and MDSU-C (N_D), and equal number of UL RRH (N_U) in both cases. The maximum number of UL UE can be served by FD C-RAN in MDSU-C scenario (K_{U_C}) is larger than or equal to that in MDSU-NC scenario ($K_{U_{NC}}$), i.e., $K_{U_C} \geq K_{U_{NC}}$

Proof : It is assumed that the number of DL RRH is equal in both MDSU-NC and MDSU-C; while that UL-RRH is also equal in both cases. From the proof of Theorem 3 under MDSU scenario, it can be seen that $K_{U_{NC}} \leq N_U - N_D\lambda$ and $K_{U_C} \leq N_U - N_D$. With $\lambda \geq 1$, it can obviously be obtained that $K_{U_C} \geq K_{U_{NC}}$, which completes the proof. ■

As can be seen from Theorem 4, the total number of UL UE is increased in MDSU-C compared to MDSU-NC. Consequently, the total UL capacity is improved when the antenna correlation exists.

B. Improvement of DL Capacity

On the other hand, the asymmetric traffic property of the optimization problem in (22) allows the system to allocate the remaining RRHs as DL RRHs once the QoS requirement in (22e) is satisfied. The comparison of maximum number of DL RRH that the system can allocate when constraint (22e) is satisfied in both MDSU-NC and MDSU-C is provided as follows.

Theorem 5 Assuming the QoS requirement of UL UEs can be satisfied with N_U^{req} UL RRHs. The maximum number of DL RRHs that FD C-RAN can allocate for DL UEs in MDSU-C (N_{D_C}) is larger than or equal to that in MDSU-NC ($N_{D_{NC}}$), i.e., $N_{D_C} \geq N_{D_{NC}}$.

Proof : According to inequality (53b), the maximum number of DL RRH that FD C-RAN can allocate to the DL UEs in the MDSU-NC and MDSU-C are limited by the number UL RRH and UL UE and can be written as $N_{D_{NC}} \leq \frac{N_U^{\text{req}} - K_U}{\lambda}$, and $N_{D_C} \leq N_U^{\text{req}} - K_U$. Since $\lambda \geq 1$, it is obvious that $N_{D_C} \geq N_{D_{NC}}$, which completes the proof. ■

In addition to comparing the number of DL RRH in MDSU-NC and MDSU-C, the capacities of k -th DL UE in these two cases are also compared and the result is provided as follows.

Corollary 2 Under high SNR condition, the capacity of k -th DL UE in the MDSU-C (C_{C_k}) is higher than that in MDSU-NC (C_{NC_k}), i.e., $C_{C_k} \geq C_{NC_k}$.

Proof : Based on Theorem 5, the capacity of k -th DL UE in the MDSU-NC and MDSU-C can be respectively written as

$$C_{Z_k} = \log_2 \left(1 + \frac{\sum_{i=1}^{N_{D_Z}} p_{M_{i,k}} \|\mathbf{g}_{D_{i,k}}^H\|^2}{\sum_{i=1}^{N_{D_Z}} \sum_{j=1, j \neq k}^{K_D} p_{M_{i,j}} \|\mathbf{g}_{D_{i,k}}^H\|^2 + \sigma_k^2} \right), \quad (56)$$

with $Z \in \{\text{C, NC}\}$. By using the parallel decomposition formula [32, p. 301], C_{Z_k} can be rewritten as

$$\begin{aligned} C_{Z_k} &= \sum_{i=1}^{N_{D_Z}} \log_2 \left(1 + \frac{p_{M_{i,k}} \rho_{i,k}^2}{\sum_{j=1, j \neq k}^{K_D} p_{M_{i,j}} \rho_{i,k}^2 + \sigma_k^2} \right) \quad (57) \\ &\stackrel{(a)}{\approx} \sum_{i=1}^{N_{D_Z}} \log_2 \left(1 + \frac{p_{M_{i,k}} \rho_{i,k}^2}{\sum_{j=1, j \neq k}^{K_D} p_{M_{i,j}} \rho_{i,k}^2} \right), \end{aligned}$$

where $\rho_{i,k} = \phi_{NC_{i,k}}$ in MDSU-NC and $\rho_{i,k} = \phi_{C_{i,k}}$ in MDSU-C scenario respectively, which are singular values of the channel vector between i -th MA-RRH and k -th DL UE in the MDSU-NC and MDSU-C. Note that the approximation (a) and are based on the high SNR assumption. Thus, the denominator of (57) is dominated by the IUI. Since $N_{D_C} \geq N_{D_{NC}}$, the proof is completed. ■

Furthermore, when the number of DL RRH in the MDSU-NC and MDSU-C is the same, antenna correlation is still possible to be a beneficial factor for the system performance. The comparison of such scenario is provided as follows.

Theorem 6 Consider the data symbol is transmitted through broadcast channel, i.e., DL RRHs transmit the same data to DL UEs, and the number of DL RRHs in both MDSU-C and MDSU-NC are equal (N_d). The capacity of k -th DL UE in MDSU-C (C'_{C_k}) is higher than that in MDSU-NC (C'_{NC_k}), i.e., $C'_{C_k} \geq C'_{NC_k}$.

Proof : When DL RRHs transmits same data to DL UEs, the capacity of k -th DL UE in both MDSU-NC and MDSU-C will not be affected by the IUI. The achievable

capacity R_{D_k} can be rewritten as

$$C'_{Z_k} = \log_2 \left(1 + \frac{\sum_{i=1}^{N_d} p_{M_{i,k}} \|\mathbf{g}_{D_{i,k}}^H\|^2}{|I_{\text{CCI},k}|^2 + \sigma_k^2} \right). \quad (58)$$

Since the power of CCI and noise will not be different in MDSU-C and MDSU-NC scenario, it can be seen that

$$C'_{Z_k} \propto \sum_{i=1}^{N_d} \log_2 \left(1 + p_{M_{i,k}} \rho_{i,k}^2 \right), \quad (59)$$

by using the parallel decomposition formula [32, p. 301]. $\rho_{i,k}$ is defined in the same manner as that in Corollary 2, i.e., $\rho_{i,k} = \phi_{NC_{i,k}}$ in MDSU-NC and $\rho_{i,k} = \phi_{C_{i,k}}$ in MDSU-C scenario respectively, which are singular values of the channel vector between i -th MA-RRH and k -th DL UE in the MDSU-NC and MDSU-C. Since the singular value of the correlation matrix has the property that [33, Theorem 2] $\phi_{C_{i,k}} \geq \phi_{NC_{i,k}}$, $\forall i, k$. Therefore, it is obvious to acquire from expression of C'_{Z_k} and singular value property of correlation matrix that MDSU-C can achieve higher capacity than that in MDSU-NC scenario, which completes the proof. ■

V. PERFORMANCE EVALUATION

In this section, we evaluate the system performance of both proposed EFSC and GRA algorithms along with impact of antenna correlation via simulations. Parameter setting is adopted from [1, 8, 34] in this paper. Considering the FD C-RAN system with a square coverage area of $1 \times 1 \text{ km}^2$ where all the RRHs and UEs are uniformly distributed within the serving area. The maximum transmission power of RRHs and UL UEs are $p_{M_{\max}} = 46 \text{ dBm}$, $p_{S_{\max}} = 40 \text{ dBm}$ and $p_{U_{\max}} = 23 \text{ dBm}$. The pathloss effect in $\mathbf{g}_{D_{i,k}}$ and $\mathbf{g}_{D_{i,k}}^H$ can be written as $s_{i,k} = 10^{-PL_{\text{NLOS}}/10}$ where pathloss model for non-line-of-sight (NLOS) PL_{NLOS} (in dB) is $PL_{\text{NLOS}} = 145.4 + 37.5 \log_{10} d_{i,k}$. $d_{i,k}$ is the distance between the i -th SA-RRH or MA-RRH and k -th DL UE (in km). Moreover, the main system parameters such as system bandwidth, carrier frequency noise power are set to 10 MHz, 2 GHz and $N_0 = -174 \text{ dBm}$ respectively. Note that there are $K_U = 2$ UL UEs, $K_D = 2$ DL UEs, 8 SA-RRHs as UL RRHs and 4 SA-RRHs as DL RRHs in the system unless otherwise specified.

A. Performance of EFSC Scheme

In Fig. 3, we study the SINR of UL UEs versus the SI power under two different transmission power of UL UEs, i.e., $p_{U_i} = 18$ and 20 dBm . For the sake of performance comparison, EFSC under imperfect UL CSI with estimation error ratio 0.3 and two additional interference cancellation methods are also implemented as follows. Perfect cancellation of SI (PCSI) is set as an upper bound, which means that the SI can be completely eliminated while the power of intended signals from UL UEs and noises remain unchanged. Furthermore, singular

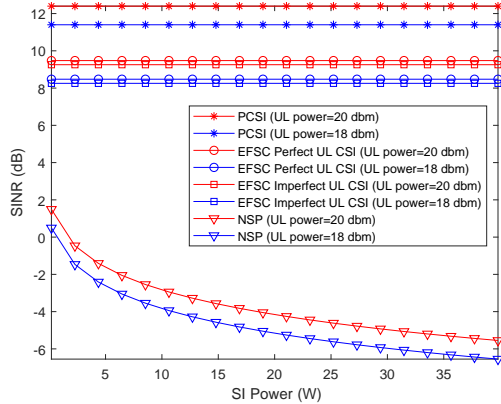


Fig. 3. SINR (dB) versus SI power (W).

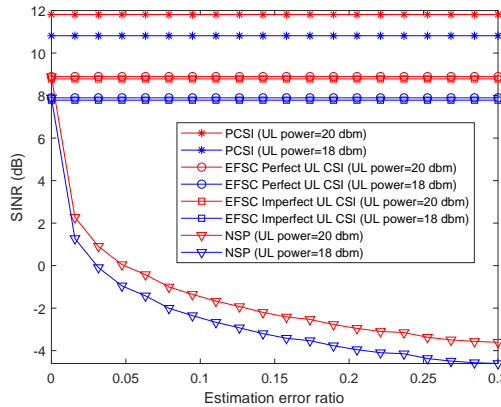


Fig. 4. SINR (dB) versus the SI channel estimation error ratio.

value decomposition (SVD)-based null space projection (NSP) coding scheme [35] is also compared and assumed to have SI channel estimation error ratio equal to 0.1. Note that definition of estimation error ratio is provided in Section II. It can be observed that when the transmission power p_{U_i} is increased, the SINR will also be enlarged, i.e., higher capacity can be achieved for UL UEs. Moreover, the SINR provided by the proposed EFSC will remain unchanged as SI power increases, which is mainly due to its advanced interference nulling procedure. The performance gaps between EFSC under perfect UL CSI and PCSI only come from noises amplified by postcoding, which cannot be eliminated. In addition, the proposed EFSC scheme can effectively eliminate SI as long as the subspace of estimated UL CSI and SI CSI are disjoint with each other. Hence, it can be seen that the proposed EFSC scheme only suffers slight performance degradation with imperfect UL CSI due to additional noise amplification and imperfect UL channel recovery. On the contrary, the SINR of NSP coding scheme will severely be degraded as SI power increases, which shows that the SVD-based coding scheme is not robust enough

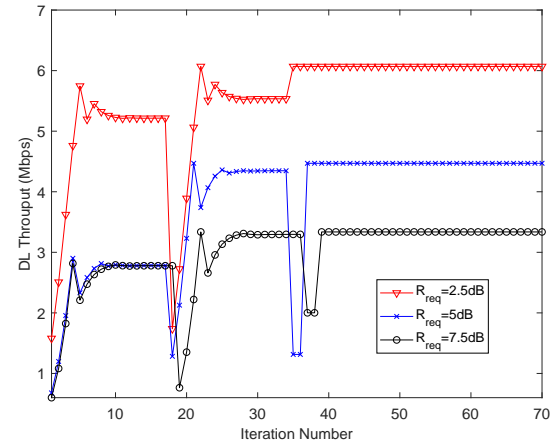


Fig. 5. Convergence of proposed GRA algorithm under different UL QoS requirement.

against interference. The robustness of designed EFSC scheme over NSP method lies in its ability of extracting essential information $\mathbf{R}_F = \mathbf{R}_y - N_0 \mathbf{I}_{N_r}$ in the received signals to acquire \mathbf{R}_F^\dagger for the construction of postcoder $\mathbf{W} = \mathbf{G}(\mathbf{G}^H \mathbf{R}_F^\dagger \mathbf{G})^{-1} \mathbf{G}^H \mathbf{R}_F^\dagger$ which only requires the statistical information of AWGN N_0 . In comparison, the NSP method requires accurate estimation of Gaussian random variable for effective SI cancellation instead of only statistical information, which makes NSP method suffer from performance degradation when channel estimation error is induced by MMSE estimator.

In Fig. 4, we investigate the SINR of UL UEs versus the SI channel estimation error ratio with SI power fixed at 40 dBm. It is observed that when estimation error ratio increases, the SINR provided by NSP coding scheme will decrease rapidly. Even when the estimation error ratio is less than 0.05, the proposed EFSC method can outperform the NSP coding scheme for more than 5 dB. Furthermore, the EFSC scheme can maintain the same SINR even with imperfect UL CSI as the estimation error ratio increases since it is not required to obtain the SI channel information while establishing the postcoding matrix. The reason for performance gaps between EFSC and PCSI schemes is similar to that in Fig. 3 from the noises amplified by postcoding.

B. Performance of GRA Algorithm

In Fig. 5, the algorithm convergence of proposed GRA scheme under different UL QoS requirement is illustrated by studying the throughput of DL UEs versus iteration number. The distances between DL UEs and UL UEs are 70 m. Note that dramatic throughput decrease happens in the case that the algorithm found the new antenna selection result when solving the master problem. Moreover, with higher QoS requirement, UL UE will have to transmit more power to achieve QoS requirement, which will lead to more CCI to DL UEs. Thus, the throughput

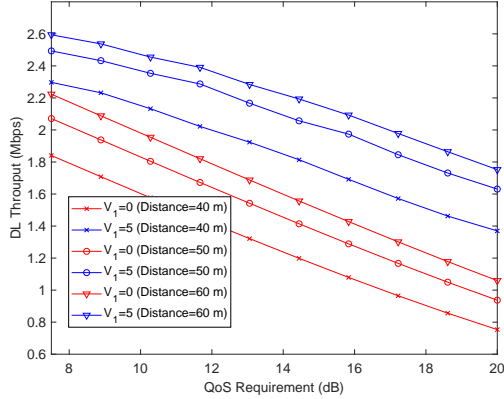


Fig. 6. Throughput versus QoS requirement.

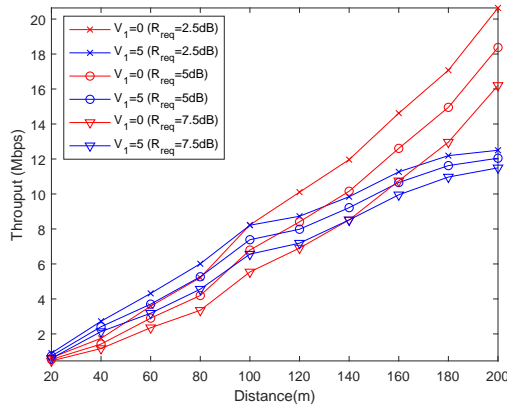


Fig. 7. Throughput versus distances.

of DL UEs will be decreased. It can be observed that the GRA algorithm can be converged within 50 iterations, which will be adopted by proposed GRA scheme in the remaining performance comparisons.

Fig. 6 shows the DL throughput performance of proposed GRA algorithm versus QoS requirements of UL UEs under different distances between UL UEs and DL UEs. Note that the parameter V_1 is defined in the utility function in \mathcal{U}_S considering the tradeoff between DL capacity and CCI, i.e., $V_1 = 0$ assumes non-existence of CCI while $V_1 = 5$ denotes certain level of CCI in the network. It can be observed that with higher UL QoS requirement, UL UE has to transmit more power to achieve the guaranteed QoS, which will lead to increasing power of CCI and degrade throughput of DL UEs. Moreover, since the designed utility function considers the quality of DL channel and influence of CCI simultaneously, the proposed GRA method with parameter $V_1 = 5$ achieves higher throughput than that with $V_1 = 0$ under different QoS requirement.

In Fig. 7, we study the distance between UL UEs and DL UEs versus the throughput of DL UEs under different QoS requirement R_{req} with $V_1 = 0$ and 5. It can be seen

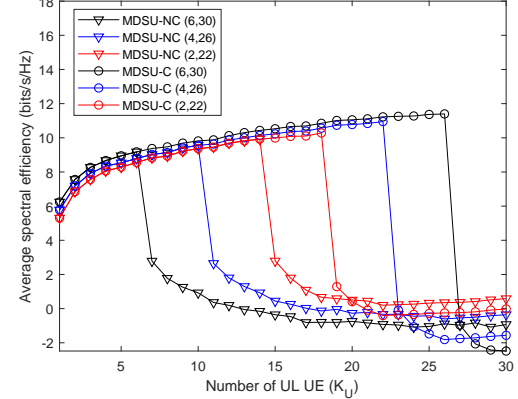


Fig. 8. Average spectrum efficiency versus number of UL UE.

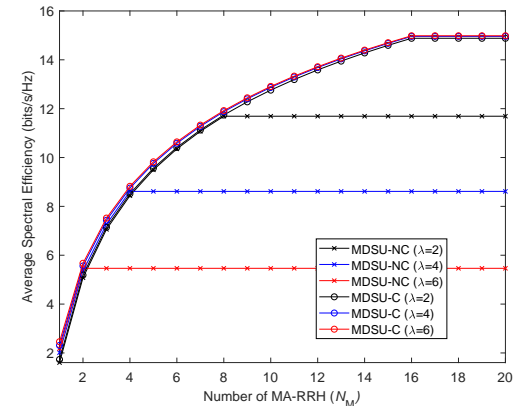


Fig. 9. Average spectrum efficiency versus number of MA-RRH.

that with decreased distance, the CCI caused from UL UEs to DL UEs will be augmented, which consequently degrades the DL throughput. Moreover, when the distance between DL UEs and UL UEs are more than a certain value, e.g., 80 m with $R_{\text{req}} = 2.5$ dB, the antennas selected to maximize DL channel quality ($V_1 = 0$) will have better throughput than that considering the influence of CCI ($V_1 = 5$). On the contrary, when the distance is less than 80 m, the power of CCI from UL UEs to DL UEs will significantly increase and dominate the throughput of DL UEs. Consequently, the GRA algorithm with $V_1 = 5$ achieves higher throughput than that with $V_1 = 0$. This flexibility to adjust parameter V_1 allows our proposed GRA algorithm to provide balance of tradeoff between DL throughput and CCI under various scenarios.

C. Impact of Antenna Correlation

Fig. 8 shows the improvement of UL capacity from antenna correlation by illustrating the average spectrum efficiency of UL UE versus number of UL UE K_U for MDSU-NC and MDSU-C cases. The total number of antennas is fixed and the ratio between number of

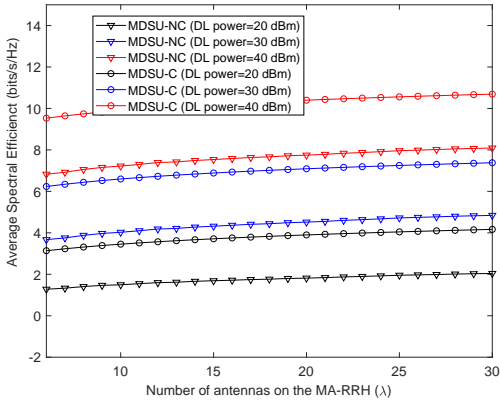


Fig. 10. Average spectrum efficiency versus number of antennas on the MA-RRH.

transmit antenna and receive antenna is compared in three different patterns, i.e., the number of antenna on the MA-RRH and the number of SA-RRH are chosen as $(\lambda, N_S) = (6, 30)$, $(4, 26)$ and $(2, 22)$. The number of MA-RRH and number of DL UE are $N_M = 4$ and $K_D = 4$, respectively. The transmission power of UL UE is fixed at 20 dBm. To ensure that subspaces spanned by UL and SI channel are disjoint with each other, constraint (53b) should be satisfied. It means that the maximum number of UL UE the FD C-RAN can serve is limited by the rank of UL channel (N_U), rank of SI channel ($N_D \lambda$ in MDSU-NC and N_D in MDSU-C) as shown in Proof of Theorem 4. It can be seen from Fig. 8 that when number of UL UE exceeds a certain value, which violates constraint (53b), the subspaces of UL channel and SI channel will overlap such that SI cannot be eliminated completely. Consequently, the average spectrum efficiency drops dramatically. Moreover, since the rank of SI channel is reduced by antenna correlation from $N_D \lambda$ to N_D , the MDSU-C scenario will be able to serve more UL UE than that for MDSU-NC. For example, when $(\lambda, N_S) = (6, 30)$, the rank of SI channel is 24 in MDSU-NC scenario, which means the number of UL UE should not exceed 6 in order to eliminate SI. Hence, the average spectrum efficiency for MDSU-NC case is severely decreased at $K_U = 7$. On the contrary, the rank of SI channel is reduced to 4 by antenna correlation in MDSU-C scenario, which indicates the number of UL UE should not exceed 26. Therefore, the average spectrum efficiency in MDSU-C scenario does not suffer from degradation until $K_U = 27$. The correctness of Theorem 4 can therefore be verified by Fig. 8.

In Fig. 9, the improvement of DL capacity from antenna correlation is shown by studying the average spectrum efficiency of DL UE for MDSU-NC and MDSU-C versus the number of MA-RRH N_M . Different antenna numbers, $\lambda = 2, 4$, and 6 , on each MA-RRH are also compared when QoS requirement of UL UEs is satisfied

by $N_U^{\text{req}} = 18$ SA-RRHs. Similar to the reason as stated in Fig. 8, the maximum number of RRH that FD C-RAN can allocate for DL communications is limited by the rank of UL channel (N_U^{req}), the rank of SI channel ($N_{D_{NC}} \lambda$ in MDSU-NC and N_{D_C} in MDSU-C) and the number of UL UE (K_U) as shown in Proof of Theorem 5. Hence, the average spectrum efficiency will remain constant after the number of MA-RRH exceed a certain value to satisfy constraint (53b). Moreover, since the rank of SI channel is reduced by antenna correlation from $N_{D_{NC}} \lambda$ to N_{D_C} , it can be seen that the number of RRH that the entire C-RAN can allocate in MDSU-C case is larger than that in MDSU-NC. Verification of Theorem 5 is consequently attained in this figure.

Fig. 10 shows the improvement of DL capacity from antenna correlation when the DL RRHs transmit same data to the DL UEs by observing the average spectrum efficiency of DL UEs versus number of antennas on the MA-RRH λ . Both for MDSU-NC and MDSU-C cases are compared under different transmission power of MA-RRH with $N_M = 1$. It can be seen that when λ is increased, the system can achieve higher average spectrum efficiency for DL communications. Moreover, the MDSU-C case can provide higher spectrum efficiency compared to MDSU-NC since the channel in MDSU-C possesses larger singular value [33, Theorem 2]. The feasibility of Theorem 6 is verified by Fig. 10.

VI. CONCLUSIONS

In this paper, we study joint interference cancellation and resource allocation for FD C-RAN with antenna correlation. The optimization problem is formulated with consideration of asymmetric traffic type in practical system. To deal with high coupling between variables for RRH selection and postcoding, we first propose an EFSC method with the advantage of reducing signaling overhead for channel estimation to tackle the SI problem in the considered system. The reduced signaling overhead and capacity improvement is derived in mathematical formula explicitly. Moreover, the proposed GRA scheme considers the tradeoff between DL capacity and CCI by separately optimizing the continuous and discrete variables and a well-designed utility function. Furthermore, we identify the scenario in which antenna correlation is beneficial for UL and DL communications along with the associated derivation. Performance evaluation shows the effectiveness of proposed schemes as well as the insights of antenna correlation to resource allocation strategies for FD C-RAN.

APPENDIX A PROOF OF THEOREM 1

For detailed concept of proposed EFSC scheme, please refer to [36, 37]. Due to space limitation, we will only present how to obtain $\mathbf{W} = \mathbf{G}\bar{\mathbf{G}}$, with $\bar{\mathbf{G}} =$

$(\mathbf{G}^H \mathbf{Q}_{\mathcal{H}}^\perp \mathbf{G})^{-1} \mathbf{G}^H \mathbf{Q}_{\mathcal{H}}^\perp$ and $\mathbf{Q}_{\mathcal{H}}^\perp = \mathbf{I} - \mathbf{H}(\mathbf{H}^H \mathbf{H})^{-1} \mathbf{H}^H$ when only UL CSI is available. The following Lemma is introduced to prove Theorem 1.

Lemma 1

- (a) $\bar{\mathbf{G}}\mathbf{G} = \bar{\mathbf{H}}\mathbf{H} = \mathbf{I}$.
- (b) $\bar{\mathbf{G}}\mathbf{H} = \bar{\mathbf{H}}\mathbf{G} = \mathbf{0}$.
- (c) The pseudo inverse of $\mathbf{F} = [\mathbf{G} \quad \mathbf{H}]$ can be expressed as $\mathbf{F}^\dagger = (\mathbf{F}^H \mathbf{F})^{-1} \mathbf{F}^H = [\bar{\mathbf{G}} \quad \bar{\mathbf{H}}]^T$, with $\bar{\mathbf{H}} = (\mathbf{H}^H \mathbf{Q}_{\mathcal{G}}^\perp \mathbf{H})^{-1} \mathbf{H}^H \mathbf{Q}_{\mathcal{G}}^\perp$ and $\mathbf{Q}_{\mathcal{G}}^\perp = \mathbf{I} - \mathbf{G}(\mathbf{G}^H \mathbf{G})^{-1} \mathbf{G}^H$.

Proof:

- (a) $\bar{\mathbf{G}}\mathbf{G} = (\mathbf{G}^H \mathbf{Q}_{\mathcal{H}}^\perp \mathbf{G})^{-1} \mathbf{G}^H \mathbf{Q}_{\mathcal{H}}^\perp \mathbf{G} = \mathbf{I}$. A similar proof can be applied to show that $\bar{\mathbf{H}}\mathbf{H} = \mathbf{I}$.
- (b) Since $\mathbf{Q}_{\mathcal{H}}^\perp \mathbf{H} = (\mathbf{I} - \mathbf{H}(\mathbf{H}^H \mathbf{H})^{-1} \mathbf{H}^H) \mathbf{H} = \mathbf{H} - \mathbf{H} = \mathbf{0}$. It can be seen that $\bar{\mathbf{G}}\mathbf{H} = (\mathbf{G}^H \mathbf{Q}_{\mathcal{H}}^\perp \mathbf{G})^{-1} \mathbf{G}^H \mathbf{Q}_{\mathcal{H}}^\perp \mathbf{H} = (\mathbf{G}^H \mathbf{Q}_{\mathcal{H}}^\perp \mathbf{G})^{-1} \mathbf{G}^H \mathbf{0} = \mathbf{0}$. Same result can be obtained for $\mathbf{H}\mathbf{G} = \mathbf{0}$ based on similar derivation.
- (c) Based on Lemmas 1(a) and 1(b), we can obtain that $\mathbf{F}^\dagger \mathbf{F} = [\bar{\mathbf{G}} \quad \bar{\mathbf{H}}]^T [\mathbf{G} \quad \mathbf{H}] = \begin{bmatrix} \bar{\mathbf{G}}\mathbf{G} & \bar{\mathbf{G}}\mathbf{H} \\ \bar{\mathbf{H}}\mathbf{G} & \bar{\mathbf{H}}\mathbf{H} \end{bmatrix} = \mathbf{I}$, which completes the proof. ■

From Lemma 1(c), the pseudo inverse of $\mathbf{R}_F = \mathbf{R}_y - N_0 \mathbf{I}_{N_r} = E[\mathbf{y}\mathbf{y}^H] - N_0 \mathbf{I}_{N_r} = \mathbf{F}\tilde{\mathbf{x}}\tilde{\mathbf{x}}^H \mathbf{F}^H$ can be expressed as $\mathbf{R}_F^\dagger = (\mathbf{F}^H)^\dagger \tilde{\mathbf{x}}^{-1} \mathbf{F}^\dagger$, with $\tilde{\mathbf{x}} = \tilde{\mathbf{x}}\tilde{\mathbf{x}}^H$. Multiplying \mathbf{R}_F^\dagger by \mathbf{G}^H in the left-hand side, we have

$$\mathbf{G}^H \mathbf{R}_F^\dagger = \begin{bmatrix} \mathbf{I}_{N_r} \\ \mathbf{0} \end{bmatrix}^H \tilde{\mathbf{x}}^{-1} \begin{bmatrix} \bar{\mathbf{G}} \\ \bar{\mathbf{H}} \end{bmatrix} = \tilde{\mathbf{x}}_{N_r}^{-1} \bar{\mathbf{G}}, \quad (60)$$

where $\tilde{\mathbf{x}}_{N_r}^{-1} = \begin{bmatrix} \mathbf{I}_{N_r} \\ \mathbf{0} \end{bmatrix}^H \tilde{\mathbf{x}}^{-1}$. Then, multiplying (60) by \mathbf{G} in the right-hand side, we have

$$\mathbf{G}^H \mathbf{R}_F^\dagger \mathbf{G} = \begin{bmatrix} \mathbf{I}_{N_r} \\ \mathbf{0} \end{bmatrix}^H \tilde{\mathbf{x}}^{-1} \begin{bmatrix} \mathbf{I}_{N_r} \\ \mathbf{0} \end{bmatrix} = \tilde{\mathbf{x}}_{N_r}^{-1}. \quad (61)$$

Equalities of (60) and (61) follow from Lemma 1(a) and 1(b). $\bar{\mathbf{G}}$ can be obtained as

$$(\mathbf{G}^H \mathbf{R}_F^\dagger \mathbf{G})^{-1} \mathbf{G}^H \mathbf{R}_F^\dagger = (\tilde{\mathbf{x}}_{N_r}^{-1})^{-1} \tilde{\mathbf{x}}_{N_r}^{-1} \bar{\mathbf{G}} = \bar{\mathbf{G}}. \quad (62)$$

Hence, the proposed EFSC can be constructed as

$$\mathbf{W} = \mathbf{G}(\mathbf{G}^H \mathbf{R}_F^\dagger \mathbf{G})^{-1} \mathbf{G}^H \mathbf{R}_F^\dagger. \quad (63)$$

■

REFERENCES

- [1] D. W. K. Ng, Y. Wu, and R. Schober, "Power Efficient Resource Allocation for Full-Duplex Radio Distributed Antenna Networks," *IEEE Trans. Wire. Commun.*, vol. 15, no. 4, pp. 2896–2911, Apr. 2016.
- [2] M. Duarte, C. Dick, and A. Sabharwal, "Experiment-Driven Characterization of Full-Duplex Wireless Systems," *IEEE Trans. Wire. Commun.*, vol. 11, no. 12, pp. 4296–4307, Dec. 2012.
- [3] F. Lehmann and A. O. Berthet, "A Factor Graph Approach to Digital Self-Interference Mitigation in OFDM Full-Duplex Systems," *IEEE Signal Process. Lett.*, vol. 24, no. 3, pp. 344–348, Mar. 2017.
- [4] A. Masmoudi and T. Le-Ngoc, "Channel Estimation and Self-Interference Cancelation in Full-Duplex Communication Systems," *IEEE Trans. Veh. Technol.*, vol. 66, no. 1, pp. 321–334, Jan. 2017.
- [5] D. Liu, S. Shao, Y. Shen, Q. Liang, and Z. Lu, "Analysis of Analog Self-Interference Cancellation with Imperfect Channel State Information for Full-Duplex Radios," in *IEEE Globecom*, Dec. 2016, pp. 1–6.
- [6] M. A. Ahmed, C. C. Tsimenidis, and A. F. A. Rawi, "Performance Analysis of Full-Duplex-MRC-MIMO With Self-Interference Cancellation Using Null-Space-Projection," *IEEE Trans. Signal Process.*, vol. 64, no. 12, pp. 3093–3105, Jun. 2016.
- [7] H. Q. Ngo, H. A. Suraweera, M. Matthaiou, and E. G. Larsson, "Multipair Full-Duplex Relaying With Massive Arrays and Linear Processing," *IEEE J. Sel. Areas Commun.*, vol. 32, no. 9, pp. 1721–1737, Sep. 2014.
- [8] D. Nguyen, L. N. Tran, P. Pirinen, and M. Latva-aho, "On the Spectral Efficiency of Full-Duplex Small Cell Wireless Systems," *IEEE Trans. Wire. Commun.*, vol. 13, no. 9, pp. 4896–4910, Sep. 2014.
- [9] O. Simeone, E. Erkip, and S. Shamai, "Full-Duplex Cloud Radio Access Networks: An Information-Theoretic Viewpoint," *IEEE Wire. Commun. Lett.*, vol. 3, no. 4, pp. 413–416, Aug. 2014.
- [10] M. Mohammadi, H. A. Suraweera, and C. Tellambura, "Full-Duplex Cloud-RAN with Uplink/Downlink Remote Radio Head Association," in *IEEE ICC*, May. 2016, pp. 1–6.
- [11] M. Mohammadi, C. Tellambura, and A. Suraweera, "Uplink and Downlink Rate Analysis of a Full-Duplex C-RAN with Radio Remote Head Association," in *Proc. EUSIPCO*, Aug. 2016, pp. 778–782.
- [12] P. R. Li and K. T. Feng, "Channel-aware resource allocation for energy-efficient cloud radio access networks under outage specifications," *IEEE Trans. Wire. Commun.*, vol. 16, no. 11, pp. 7389–7403, Nov. 2017.
- [13] P. R. Li, T. S. Chang, and K. T. Feng, "Energy-efficient power allocation for distributed large-scale mimo cloud radio access networks," in *IEEE WCNC*, Apr. 2014, pp. 1856–1861.
- [14] S. Jang, M. Ahn, H. Lee, and I. Lee, "Antenna Selection Schemes in Bidirectional Full-Duplex MIMO Systems," *IEEE Trans. Veh. Technol.*, vol. 65, no. 12, pp. 10 097–10 100, Dec. 2016.
- [15] Z. Liu, Y. Liu, and F. Liu, "Fast Antenna Selection Algorithm for Full-Duplex MIMO Communication System," in *IEEE/CIC ICCC*, Nov. 2015, pp. 1–5.
- [16] J. Feng, S. Ma, G. Yang, and B. Xia, "Power Scaling of Full-Duplex Two-Way Massive MIMO Relay Systems with Correlated Antennas and MRC/MRT Processing," *IEEE Trans. Wire. Commun.*, vol. 16, no. 7, pp. 4738–4753, Jul. 2017.
- [17] A. Almradi and K. A. Hamdi, "Ergodic Capacity Analysis of Correlated MIMO Full-Duplex Relaying," in *IEEE ICC*, May. 2016, pp. 1–7.
- [18] C. Kim and C. Kim, "A Full-Duplex MAC Protocol for Efficient Asymmetric Transmission in WLAN," in *Proc. ICNC*, Feb. 2016, pp. 1–5.
- [19] H. Malik, M. Ghorashi, and R. Tafazolli, "Cross-Layer Approach for Asymmetric Traffic Accommodation in Full-Duplex Wireless Network," in *Proc. EuCNC*, Jun. 2015, pp. 265–269.
- [20] M. A. Alim and T. Watanabe, "Full-Duplex Medium Access Control Protocol for Asymmetric Traffic," in *IEEE VTC-Fall*, Sep. 2016, pp. 1–6.
- [21] J. Liu, S. Han, W. Liu, Y. Teng, and N. Zheng, "Performance Gain of Full-Duplex over Half-Duplex under Bidirectional Traffic Asymmetry," in *IEEE ICC*, May. 2016, pp. 98–103.
- [22] G. Strang, *Introduction to Linear Algebra*, 4th ed. Wellesley, MA: Wellesley-Cambridge Press, 2009.
- [23] T. L. Marzetta, "Noncooperative Cellular Wireless with Unlimited Numbers of Base Station Antennas," *IEEE Trans. Wire. Commun.*, vol. 9, no. 11, pp. 3590–3600, Nov. 2010.
- [24] C. A. Floudas, "Non-Linear and Mixed-Integer Optimization: Fundamentals and Applications," in *New York: Oxford University Press*, 1995.
- [25] M. L. J. W. Hemmecke, Raymond Kppe and Robert, "Non-Linear Integer Programming," in *Springer*, 2010.
- [26] Z. Quan, M. Zhu, and S. Cui, "A Fast Receiver Sensitivity Identification Method for Wireless Systems," in *IEEE ICC*, May. 2016, pp. 1–6.
- [27] J. Li and A. P. Petropulu, "A Low Complexity Algorithm for Collaborative-Relay Beamforming," in *IEEE ICASSP*, May. 2013, pp. 5002–5005.

- [28] F. Fang, H. Zhang, J. Cheng, and V. C. M. Leung, "Energy Efficiency of Resource Scheduling for Non-Orthogonal Multiple Access (NOMA) Wireless Network," in *IEEE ICC*, May. 2016, pp. 1–5.
- [29] B. Khamidehi, A. Rahmati, and M. Sabbaghian, "Joint Sub-Channel Assignment and Power Allocation in Heterogeneous Networks: An Efficient Optimization Method," *IEEE Commun. Lett.*, vol. 20, no. 12, pp. 2490–2493, Dec. 2016.
- [30] M. ApS, *The MOSEK Optimization Toolbox for MATLAB Manual. Version 7.1 (Revision 28)*, 2015. [Online]. Available: <http://docs.mosek.com/7.1/toolbox/index.html>
- [31] I. Gurobi Optimization, "Gurobi Optimizer Reference Manual," 2016. [Online]. Available: <http://www.gurobi.com>
- [32] A. Goldsmith, *Wireless Communications*. New York, NY, USA: Cambridge University Press, 2005.
- [33] H. Wang, P. Wang, and L. Ping, "On the Capacity Gain from Antenna Correlation in Multi-User MIMO Systems," in *IEEE ICC*, Jun. 2012, pp. 3878–3883.
- [34] 3GPP, *Evolved Universal Terrestrial Radio Access (E-UTRA); Further Advancements for E-UTRA Physical Layer Aspects*, 2010, no. TR36.814, v9.0.0.
- [35] M. A. Ahmed, C. C. Tsimenidis, and A. F. A. Rawi, "Performance Analysis of Full-Duplex-MRC-MIMO With Self-Interference Cancellation Using Null-Space-Projection," *IEEE Trans. Signal Process.*, vol. 64, no. 12, pp. 3093–3105, Jun. 2016.
- [36] C. H. Fang, P. R. Li, and K. T. Feng, "Oblique Projection-based Interference Cancellation in Full-Duplex MIMO Systems," in *IEEE ICC*, May. 2016, pp. 1–5.
- [37] R. T. Behrens and L. L. Scharf, "Signal Processing Applications of Oblique Projection Operators," *IEEE Trans. Signal Process.*, vol. 42, no. 6, pp. 1413–1424, Jun. 1994.



Kai-Ten Feng received the B.S. degree from the National Taiwan University, Taipei, Taiwan, in 1992, the M.S. degree from the University of Michigan, Ann Arbor, in 1996, and the Ph.D. degree from the University of California, Berkeley, in 2000.

Since August 2011, he has been a full Professor with the Department of Electrical and Computer Engineering, National Chiao Tung University (NCTU), Hsinchu, Taiwan, where he was an Associate Professor and Assistant Professor from August 2007 to July 2011 and from February 2003 to July 2007, respectively. He served as the Associated Dean of Electrical and Computer Engineering College at NCTU starting from February 2017. From July 2009 to March 2010, he was a Visiting Research Fellow with the Department of Electrical and Computer Engineering, University of California at Davis. Between 2000 and 2003, he was an In-Vehicle Development Manager/Senior Technologist with OnStar Corporation, a subsidiary of General Motors Corporation, where he worked on the design of future Telematics platforms and in-vehicle networks. His current research interests include broadband wireless networks, cooperative and cognitive networks, smart phone and embedded system designs, wireless location technologies, and intelligent transportation systems.

Dr. Feng received the Best Paper Award from the Spring 2006 IEEE Vehicular Technology Conference, which ranked his paper first among the 615 accepted papers. He also received the Outstanding Youth Electrical Engineer Award in 2007 from the Chinese Institute of Electrical Engineering, and the Distinguished Researcher Award from NCTU in 2008, 2010, and 2011. He has been serving as the technical advisor for IEEE-HKN honor society and National Academy of Engineering (NAE) grand challenges scholars program (GCSP) at NCTU since 2018. He has also served on the technical program committees in various international conferences.


Chun-Hao Fang received the BS degree in 2014 from the department of Electrical and Computer Engineering, National Chiao Tung University, Hsinchu, Taiwan. Since 2014, he has been working toward the PhD degree in the Institute of Communications Engineering, National Chiao Tung University. His research interests include interference cancellation, resource allocation design for full-duplex, cloud radio access networks, and 5G networks.


Pei-Rong Li received the B.S. degree from the department of Communications Engineering, Yuan Ze University, Taoyuan, Taiwan, in 2012. She was a visiting scholar at Department of Electrical and Computer Engineering, University of California at Davis, Davis, CA, USA, from Mar. 2017 to Nov. 2017. She also visited 5GIC center in University of Surrey, UK, from July 2017 to Aug. 2017. She received the Ph.D. degree in the Institute of Communications Engineering, National Chiao Tung University, Hsinchu, Taiwan. Her research interests are in the areas of wireless communications including radio resource management, functional splitting, and network slicing technologies for 5G networks. She is also working on signal processing for wireless communications with special emphasis on joint design of detection and decoding.